# Transient simulation of graphene FET gated by electrolyte medium

Koki Arihori, Matsuto Ogawa and Satofumi Souma†
Department of Electrical and Electronic Engineering,
Kobe University, Kobe 657-8501, Japan
†email: ssouma@harbor.kobe-u.ac.jp

Junko Sato-Iwanaga and Masa-aki Suzuki
Innovation Promotion Sector, Panasonic Corporation,
Osaka 571-8508, Japan

***Abstract*—We present a numerical study on the electrical conduction characteristics of the graphene channel FET with electrolyte medium for gate control. By using the tight-binding formalism to calculate the electronic band structure and the Nernst-Planck-Poisson (NPP) equation to calculate the formation of the electric double layer at the interface of the ionic liquid, we found that the drain current after the EDL is formed is almost independent of the IL thickness, while the transient behavior is greatly influenced by the thickness of ionic liquid. In addition, we present our simulation results for the case of solid electrolyte gate, where the effect of finite ion concentration in the solid electrolyte has been successfully taken into account appropriately by using the extended NPP equation.**

## I. Introduction

Graphene has been considered as an attractive material for the nanoelectronics applications [1]. Here the wide range of controllability in the electric field applied to graphene is an important issue in realizing wide range of controllability in carrier concentration and electronic current.

Among various approaches to apply electric field to graphene, including traditional top gating via gate insulator, the use of electrolyte medium [i.e., ionic liquid (IL) or ionic solid (IS)] is beneficial in obtaining high carrier density in graphene, where the formation of an electric double layer (EDL) with the thickness $\sim$ 1 nm at the electrolyte medium/graphene interface is essential in inducing high electric field and consequently a high density of carriers [2], [3], [4], [5]. However, it has not been explored theoretically enough in how the thicknesses, ion concentrations, and the diffusion coefficients of IL and IS play the roles in the resulting electronic current flowing through graphene. With such motivation, we present a numerical study on the electrical conduction characteristics of the graphene channel FET using electrolyte medium for gate control.

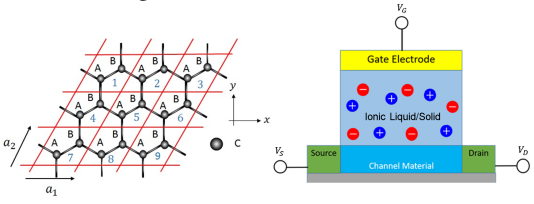


Fig. 1. (Left): Crystal structure of graphene. (Right): Schematic illustration of IL gated graphene FET.

## II. Theoretical formalism

### A. Tight-binding (TB) formalism

In Fig. 1 we show the schematic illustration of the device structure considered in this study, where the graphene channel part is described by the TB method and the electrolyte medium (IL or IS) part is described by the Nernst-Planck-Poisson equation. Their coupling is assumed to be electrostatic and is also described by the Poisson's equation. Electronic properties of graphene can be calculated by solving the eigenvalue problem $H(\boldsymbol{k})\,|\psi_{l\boldsymbol{k}}\rangle = E_l(\boldsymbol{k})\,|\psi_{l\boldsymbol{k}}\rangle$ [$l = 1$ (2) corresponds to the valence (conduction) band] with the Hamiltonian

$$H(\boldsymbol{k}) = \begin{pmatrix} 0 & H^*_{\rm BA}(\boldsymbol{k}) \\ H_{\rm BA}(\boldsymbol{k}) & 0 \end{pmatrix}, \quad (1)$$

$$H_{\rm BA}(\boldsymbol{k}) = -t\left(2e^{ik_y a_0/2}\cos(k_x\sqrt{3}a_0/2) + e^{-ik_y a_0}\right), \quad (2)$$

where $a_0$ is the spacing between nearest-neighbor atoms and $t = 2.7$ eV is the nearest neighbor hopping energy [6].

### B. Current calculation method under the ballistic condition

Once the band structure $E_l(\boldsymbol{k})$ is calculated, the electronic current flowing through graphene attached at both ends to ideal electrodes can be calculated as

$$I = \frac{q}{\hbar}\frac{1}{N_{\rm kp}S_{\rm UC}}\sum_l\sum_{\mathbf{k}\in{\rm BZ}}^{N_{\rm kp}}|v_l(\mathbf{k})| \times\left[f\left(E_l(\mathbf{k})+U_{\rm C}-E_{\rm FL}\right)-f\left(E_l(\mathbf{k})+U_{\rm C}-E_{\rm FR}\right)\right]. \quad (3)$$

Here $N_{\rm kp}$ is the total number of $\mathbf{k}$ sampling points within the 1st Brillouin zone (BZ), $q = -e$ is the charge of an electron, $E_l(\mathbf{k})$ and $v_l(\mathbf{k})$ are the energy and the group velocity for the energy eigenstate $|\psi_{l\mathbf{k}}\rangle$, and $f(E)$ is the Fermi distribution function, where $E_{\rm FL/FR}$ is the Fermi energy in the left/right electrode so that $V_{\rm D} = (E_{\rm FL} - E_{\rm FR})/e$ is the drain voltage, $U_{\rm C} = -e\varphi(z_{\rm gra})$ with $\varphi(z_{\rm gra})$ being the electrostatic potential at the graphene layer.

### C. Nernst-Planck-Poisson equation

The electrostatic potential $\varphi(z_{\rm gra})$ at the graphene layer, required in Eq. (3) is determined by the coupling with the

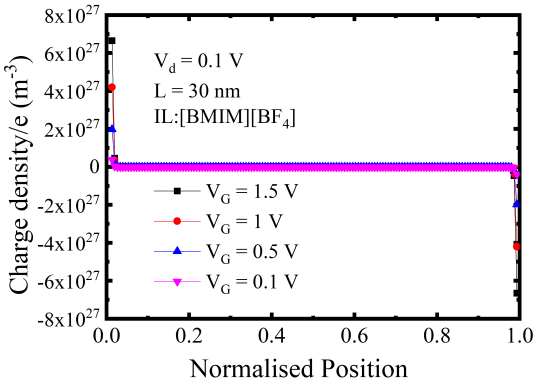


Fig. 2. Charge density in units of $e$ in the IL region of IL-gated FET for various gate voltages at the time 50 ns.

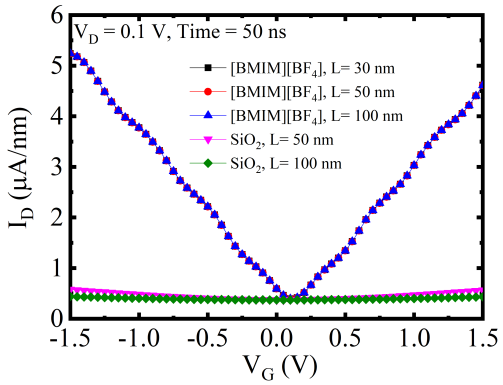


Fig. 3. $I_{\rm D}$-$V_{\rm G}$ characteristics for various thicknesses of IL as indicated in the figure at the time 50 ns for IL-gated FET. Results for the conventional FET with $SiO_2$ gate insulator with the thickness 50 nm and 100 nm are also shown for comparison.

electrolyte (IL or IS) region above graphene. The electrolyte region is described by the Nernst-Planck-Poisson equation:

$$\frac{dc_j(z,t)}{dt} = -\frac{d}{dz}F_j(z,t) + [G_j(z,t) - R_j(z,t)], \tag{4}$$

$$F_j(z,t) = -D_j\frac{dc_j(z,t)}{dz} + c_j(z,t)q_jM_j\left(-\frac{d\varphi(z,t)}{dz}\right), \tag{5}$$

$$-\frac{d}{dz}\varepsilon(z)\frac{d\varphi(z,t)}{dz} = q_+c_+(z,t) + q_-c_-(z,t) + \rho_{\rm gra}(z,t). \tag{6}$$

Here $c_j(z,t)$ is the ion density for cation/anion ($j = +/-$), $F_j(z,t)$ is the flux density along the $z$-direction, $G_j(z,t)$ and $R_j(z,t)$ are the generation and recombination rate, $\varphi(z)$ is the electrostatic potential in whole region including electrolyte (IL or IS) and graphene, $D_j$ is the diffusion coefficient, $M_j = D_j/k_BT$ is the mobility, $q_\pm = \pm e$, and $\rho_{\rm gra}(z,t)$ is the charge density within the graphene layer. We used parameter values for representative IL and IS, which are [BMIM][BF4] [7] and $LiPO_4$ [8], respectively. In the actual simulations, the ion density $c_j(z,t)$ is initially assumed to be homogeneous with the values $c_\pm = 1.6 \times 10^{27}$ m$^{-3}$ and $c_\pm = 6.51 \times 10^{27}$ m$^{-3}$ in IL ([BMIM][BF4]) and IS ($LiPO_4$), respectively. We also note that, in the case of IS ($LiPO_4$) only the cations ($Li^+$ ions) are mobile ions [8], and they move through a limited number of vacancies, so that the diffusion coefficient $D$ has to be generalized to take into account the maximum density $\nu$ as $D_j' = D_j/[1 - c_j(z,t)/\nu]$ [8], [9], [10], [11]. We assume $\nu = 7.0 \times 10^{27}$ m$^{-3}$ for IS throughout this paper.

## III. Results and Discussions

We first consider the case of IL-gated FET. Figure 2 shows the cation and anion density distributions in IL ($[BMIM][BF_4]$) region for various gate voltages. Here it is seen that the EDL has been formed near the IL/graphene and IL/gate electrode interfaces by applying a gate voltage, and the ion densities near the interfaces increased as the gate voltage increased.

In Fig. 3 we show the comparison of $I_{\rm D}$-$V_{\rm G}$ characteristics for various thicknesses of ionic liquid as indicated in the figure

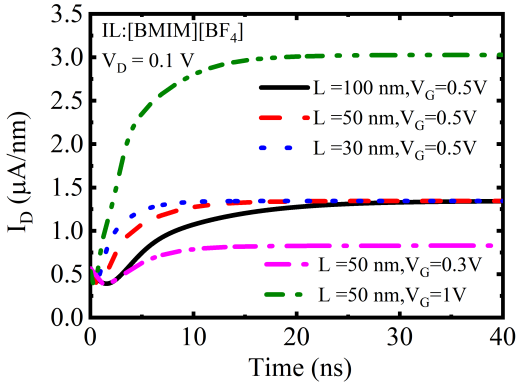


Fig. 4. Drain current $I_{\rm D}$ as a function of time for various IL thicknesses and applied gate voltages.

at the time 50 ns when the EDL formation is completed. Results for the conventional FET with $SiO_2$ gate insulator with the thickness 50 nm and 100 nm are also shown for comparison. Here it was found that the drain current when the EDL formation was completed is almost independent of the IL thickness $L$. This is a reasonable result since the thickness of the EDL is around 1 nm and the amount of charge accumulated in graphene is determined by EDL. It should be noted that the use of IL enables much larger $I_{\rm D}$ than the conventional $SiO_2$ gate insulator with the same thickness.

In Fig. 4 we compare how the transient characteristics until the EDL is formed (until the current converges) differs depending on the gate voltage and the thickness of the IL. We first observe that the initial current is independent of $L$ and $V_{\rm G}$. This is because the surface potential at the graphene is initially assumed to be zero. Importantly, the time required for the current to be saturated is longer for thicker IL thickness $L$, but is almost independent of $V_{\rm G}$. This is interpreted to be due to the longer time required for ion to move toward the interface for thicker IL.

Next we consider the case of IS-gated FET. Figure 5 shows

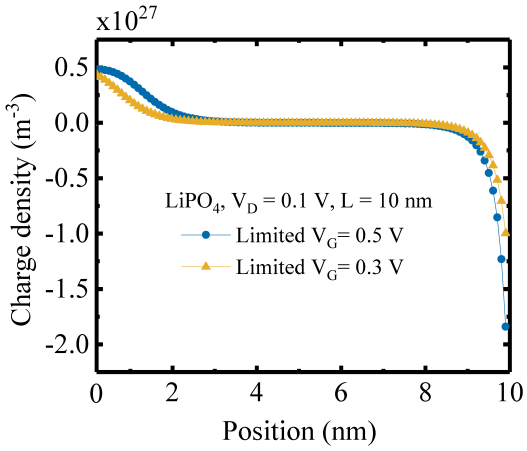


Fig. 5. Charge density distribution in units of $e$ in IS region with thickness 10 nm in IS-gate FET for various gate voltages at the time 700 $\mu$s. "Limited" stands for the limited $Li^+$ density situation imposed by the maximum density $\nu$.

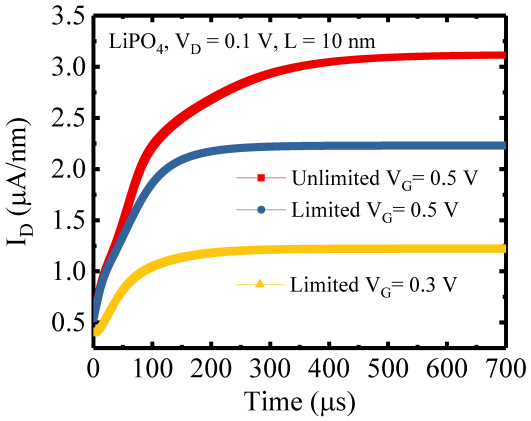


Fig. 7. Drain current $I_D$ as a function of time for various applied gate voltages for IS-gated FET.

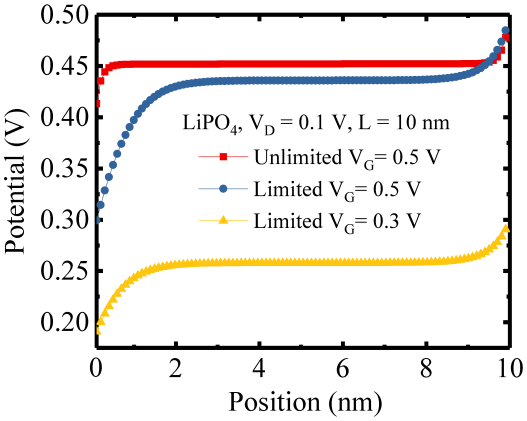


Fig. 6. Electrostatic potential distributions in IS for various gate voltages at the time 700 $\mu$s. "Limited" and "unlimited" stand for the limited and unlimited $Li^+$ density situations, where the former case the density is imposed by the maximum density $\nu$.

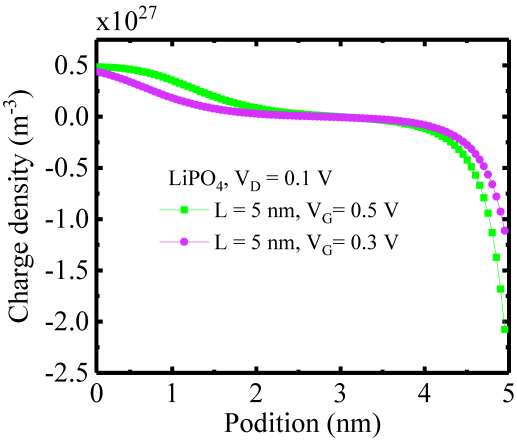


Fig. 8. Charge density in units of $e$ in IS with thickness 5 nm for various gate voltages at the time 700 $\mu$s.

the cation and anion density distributions in IS ($LiPO_4$) region for various gate voltages. Here, by applying a positive gate voltage to the IS, $Li^+$ ions start to fill up subsequently from the gate electrode side to the graphene side, and the flat charge density region (fully occupied $Li^+$ region) starts to appear near the graphene side, where the charge density at the fully occupied $Li^+$ region is determined by the imposed maximum cation density $\nu = 7.0 \times 10^{27}$ m$^{-3}$ subtracted by the homogeneous anion density $c_- = 6.51 \times 10^{27}$ m$^{-3}$. In addition, the length of the fully occupied region increases with the gate voltage. This is interpreted to be due to the movement of $Li^+$ ions through the limited numbers of vacancies.

In Fig. 6 we show the internal electrostatic potential in the IS region for various gate voltages. By placing an upper limit on the cation density (maximum density $\nu$), the potential drop in the fully occupied region (of $Li^+$ ions) becomes large compared to unlimited case, indicating that the gate electric field is screened within the fully occupied region by $Li^+$ ions and the graphene surface is not effectively influenced by the gate voltage. In addition, the potential drop in the fully occupied region becomes larger as the gate voltage increases. This is due to the fact that the length of the fully occupied region of $Li^+$ ions becomes longer as the gate voltage increases.

Figure 7 is to compare how the transient characteristics of $I_D$ are influenced by the upper limit of the ion density and value of the gate voltage through the EDL formation in IS. Here we observe that the saturated values of the drain current at around 700 $\mu$s is diminished by placing the upper limit of the ion density. This is interpreted to be due to the lower surface potential at the graphene in the limited case shown in Fig. 6. On the other hand, we can see that the current saturation time (time required for the current to be saturated) becomes shorter by placing the upper limit of the cation density. This is because in the unlimited case the $Li^+$ ions are required to reach the graphene surface to establish the steady state, while in the limited case they are allowed to move only until

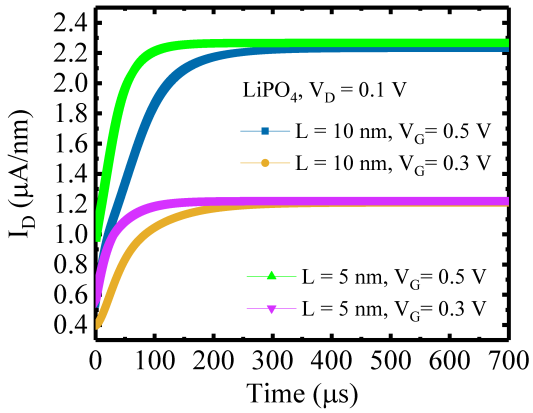


Fig. 9. Drain current $I_D$ as a function of time for various IS thicknesses and applied gate voltages.

around the edge of the fully occupied region ($\sim$ 2 nm in Fig. 6), meaning the shorter time required to establish the steady state in the limited case. Therefore the value of the saturation current and the current saturation time are in the relationship of trade-off. Moreover, we can also see that the saturation time in IS case is much longer than the IL case. This is because of the four orders of magnitude smaller values of the diffusion coefficient in IS than in IL.

In Fig. 8 we plotted the spatial distributions of charge densities in the IS region of thinner IS-gate FET with the thickness of 5 nm for two different gate voltages. Here it can be seen that the spatial extent of the region occupied fully by $Li^+$ ions is almost the same ($\sim$ 1 nm for $V_G = 0.5$ V) as for the IS thickness of 10 nm shown in Fig. 5. This observation suggests that the spatial extent of the region fully occupied by the $Li^+$ ions is determined mainly by the gate voltage. Another important observation here is that the spatial extent of the charge neutral region at around the center of IS becomes narrower as the thickness of IS decreases and the gate voltage increases. More detailed analyses for such situations including the case of extremely thinner IS will be presented elsewhere.

Finally in Fig. 9 we compare how the transient characteristics of the drain current in IS-gated FET vary with the gate voltage and the IS thickness. Important observations here are that the current saturation time is longer for thicker IS case and the saturation current value is almost independent of the IS thickness. These are the similar characteristics as in the IL-gated FET case.

## IV. Conclusion

We presented a numerical study on the electrical conduction characteristics of the graphene channel FET using electrolyte medium for gate control. By using the tight-binding formalism to calculate the electronic band structure and the Nernst-Planck-Poisson (NPP) equation to calculate the formation of the electric double layer of the ionic liquid, we found that the drain current after the EDL is formed is almost independent of the IL thickness, while the transient behavior is greatly influenced by the IL thickness $L$. Moreover, the electrical conduction characteristics of the graphene channel FET with the ionic solid gate have also been successfully studied by using the extended NPP equation, where the finite ion concentration in the solid electrolyte has been taken into account appropriately.

## Acknowledgment

This work was partially supported by JSPS KAKENHI Grant No. 19H04546.

## References

[1] K. S. Novoselov, V. I. Fal'ko, L. Colombo, P. R. Gellert, M. G. Schwab, and K. Kim, Nature, **490**, 192 (2012).
[2] X. He, N. Tang, L. Gao, J. Duan, Y. Zhang, F. Lu, F. Xu, X. Wang, X. Yang, W. Ge, and B. Shen, Appl. Phys. Lett. **104** 143102 (2014).
[3] T. Tsuchiya, K. Terabe, and M. Aono, Appl. Phys. Lett. **105**, 183101 (2014)
[4] M. Philippi, I. Gutiérrez-Lezama, N. Ubrig, and A. F. Morpurgo, Appl. Phys. Lett. **113**, 033502 (2018).
[5] A. Kumar, P. B. Pillai, X. Song, and M. M. De Souza, ACS Appl. Mater. Interfaces **10**, 19812 (2018).
[6] S. Souma, M. Ueyama and M. Ogawa, Appl. Phys. Lett. **104** 213505 (2014).
[7] S. Tsuzuki, W. Shinoda, H. Saito, M. Mikami, H. Tokuda, and M. Watanabe, J. Phys. Chem. B **113**, 10641 (2009).
[8] D. Danilov, R. A. H. Niessen, and P. H. L. Notten, J. Electorochem. Soc. **158**, A215 (2011).
[9] M. Landstorfer, S. Funken and T. Jacob, Phys. Chem. Chem. Phys. **13**, 12817 (2011).
[10] M. S. Kilic, M. Z. Bazant, A. Ajdari, Phys. Rev. E **75**, 021503 (2007).
[11] S. Braun, C. Yada, and A. Latz, J. Phys. Chem. C **119**, 22281 (2015).